Morphological Origin of Super Toughness in Poly(ethylene Terephthalate)/Polyethylene Blends

THERESA L. CARTÉ and ABDELSAMIE MOET*

Department of Macromolecular Science, Case Western Reserve University, Cleveland, Ohio 44106-7202

SYNOPSIS

A compatibilization strategy for poly(ethylene terephthalate) (PET) and polyethylene (PE) blends to achieve high toughness is described. Maleic anhydride functionalized styrene–ethylene–butylene–styrene (MA-*g*-SEBS) block copolymer at 20 pph was found to produce an intricate multidomain morphology in which the two major components (50% PE, 50% PET) and the compatibilizer coexist on a hierarchal order. A portion of the PET was dispersed as interconnected rodlike domains oriented along the injection direction. The rest of the PET and the PE constituted beadlike nano domains which served as the matrix. The blend at all these morphological levels responded to deformation in a cooperative fashion giving rise to a super tough material. That is, a blend whose elongation at break (600%) was superior to its two major components (90% for PET and 300% for PE).

INTRODUCTION

PET and PE are major contributors to the waste stream. PET and PE come from many sources such as carbonated beverage bottles, milk bottles, and other containers. Soda pop containers are comprised of PET ($\approx$ 72%) with a PE ($\approx$ 28%) base cup. Current technology to recycle these containers involves separating the two major components into pure PET and pure PE. With the recent advances in compatibilization technology, it is useful to seek a compatibilizer for these two materials in order to develop a high performance blend. In this paper, a virgin blend of PET/PE is studied to develop a compatibilization strategy to be used for the recycled blend.

PET/PE blends have been studied before with promising results in toughening the blend by compatibilization. The two major types of compatibilizers used are styrenic block copolymers and ethylene copolymers. Paul and co-workers[1] selected a styrene–ethylene–butylene–styrene (SEBS) block copolymer and an ethylene–propylene (EPDM) elastomer as compatibilizers for blends of PET/PE. They reported improved ductility with the SEBS but no significant improvement with the EPDM. Chen and Shiah[2] added an acid functionalized SEBS to bottle grade virgin materials. They found that at concentrations greater than 10% SEBS an improvement in impact strength occurred. Curry and Kiani[3] used a maleic anhydride grafted PE (MA-*g*-PE) and a styrene ethylene propylene (S–EP) block copolymer to improve the properties of recycled PET blended with HDPE basecup. The MA-*g*-PE improved compatibility slightly, and the addition of S–EP resulted in a more ductile material with good impact resistance.

Ethylene copolymers were used in the following studies. Wissler[4] examined the affect of ethylene methylacrylate, ethylene acrylic acid, and ethylene vinyl acetate copolymer modifiers and found some increase in the toughness of the recycled blends dependent on the type and amount of grafting agents in the modifier. Another study by Khelifi and Lai[5] used an ethylene vinyl acetate copolymer at 5% in various virgin PET/PE blends. They found that the compatibilizer increased the impact strength and the elongation at break without decreasing the tensile yield strength considerably.

* To whom correspondence should be addressed.

Journal of Applied Polymer Science, Vol. 48, 611–624 (1993)
 CCC 0021-8995/93/040611-14

The results from the literature show potential improvement of this blend with compatibilization. However, in the preceding studies only small increases in toughness have been achieved. Also, these results have not been studied in relation to the morphology and deformation mechanisms of the blends. It is known that the morphology affects the properties of a blend,[6] and therefore in this study a compatibilization strategy is developed based on a rational understanding of evolving morphology and deformation mechanisms. In other work, we report on the effectiveness of the results discussed here in recycled blends.[7]

MATERIALS AND TECHNIQUES

Materials

The materials used were PET, PE, and styrene–ethylene–butylene–styrene block copolymers (SEBS). The PET used was Kodapak 7352 from Eastman Chemical Co., and the HDPE was Petrothene LR 73200-00 from Quantum Chemical Co. Samples were made at compositions of 100% PET, 75 PET/25 PE, 50 PET/50 PE, 25 PET/75 PE, and 100% PE. The compatibilizers used from Shell Chemical Co. were SEBS block copolymers designated Kraton G-1650, Kraton G-1652, and Kraton FG-1901X. The major difference between the Kraton G-1650 (high viscosity SEBS) and the G-1652 (low viscosity SEBS) is their Brookfield viscosities of 8000 and 1350 cps at 77°F, respectively. The FG-1901X has similar viscosity to the G-1652, but differs from the first two by its 2% grafted maleic anhydride (MA-*g*-SEBS). Polybond 3009, which is high density polyethylene functionalized with 1% maleic anhydride (MA-*g*-PE), from BP Chemical Co. was also used. The compatibilizers were used at concentrations of 5, 10, and 20 parts per hundred (pph).

Compounding

The materials as received were dried in a vacuum oven at 100°C for 24 h. They were dry mixed and then blended using a Werner and Pfleiderer corotating, intermeshing twin screw extruder at 270°C. The extruder was operated at 200 rpm. The extrudate was cooled and stranded in a water bath before being pelletized. The pellets were injection molded into Type I tensile bars (ASTM D638). The melt temperature was 260°C, and the mold temperature was 60°C.

Mechanical Testing

The mechanical testing was done on an Instron Model 1125 using ASTM D638. The strain rate chosen to test all the materials was 100%/min. However, for an exploratory study on strain rate dependence, one composition was also run at 10%/min and 1000%/min. The calculations were done using a gauge length of 50 mm for all of the materials tested.

Morphology

The injection molded tensile bars were examined using a JEOL 840A scanning electron microscope (SEM) to determine the undeformed morphology and the mechanisms of irreversible deformation. Image analysis was used to determine the percent area of phases in some of the morphology micrographs. Differential scanning calorimetry (DSC) was carried out on a Perkin Elmer 7 Series thermal analysis system at a heating rate of 10°C/min. The samples weighed between 5 and 10 mg. Wide angle X-ray diffraction (WAXD) was used to determine the crystallinity of the materials.

RESULTS AND DISCUSSION

The mechanical properties of immiscible, uncompatibilized blends are generally known to be inferior to either of the pure components. Thus, to develop improved PET/PE blends, stress–strain analysis was conducted on compatibilized blends of each composition. The mechanical properties were determined, and, subsequently, the deformation mechanisms were identified to establish a cause–effect relationship for improved mechanical behavior.

The uncompatibilized blends of PET/PE were found to have the typical mechanical properties of immiscible blends. The modulus of PET was found to be 0.9 GPa and that of PE 0.5 GPa. The modulus at the various compositions decreased approximately linearly with increasing PE as expected, which implies that the system obeys the rule of mixtures[8] (Fig. 1). The elongations at break (ϵ_b) of the 75 PET/25 PE (7%) and the 50/50 (8%) blends were significantly inferior to either PET (90%) or PE (300%). However, the 25 PET/75 PE (140%), most likely due to the dominance of the ductile PE matrix, showed some toughness, but still fell below the average value of PET and PE (Fig. 1).

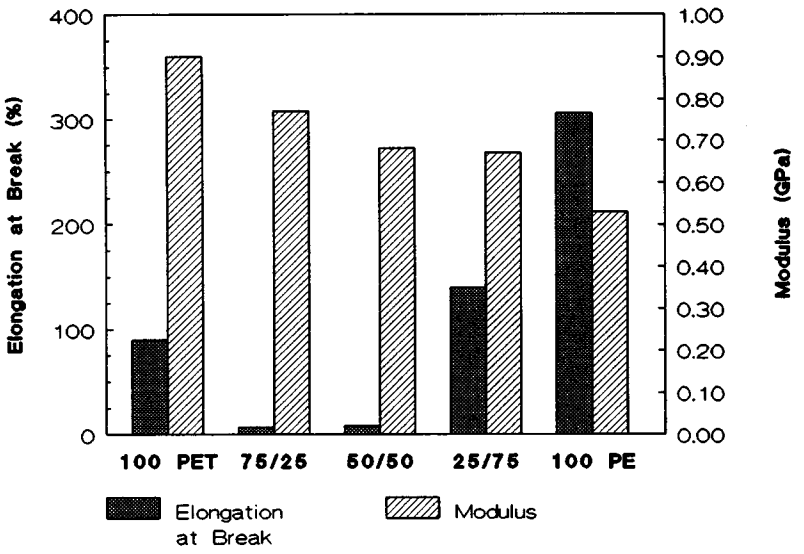

Figure 1 Mechanical properties of all compositions of PET/PE blends without compatibilizer.

Compatibilization

Recent studies[1-3] confirmed the usefulness of block copolymers as compatibilizers for immiscible polymer pairs. The block copolymer chosen should have physicochemical affinity towards both components in the blend. The general criterion is that each segment of the copolymer interacts with one of the blend components. The improved properties are commonly attributed to improved adhesion at the interface of the dispersed phase and the matrix and to a reduction in particle size.[9-11]

The large number of compositions and compatibilizers in this study necessitated limiting the variables. In order to do this, yield strength, modulus, and elongation at break were examined. The properties are discussed in relation to the amount of compatibilizer added. It was then determined which property revealed the effectiveness of compatibilization. From this it was determined which composition was most effected by compatibilization. Next, the best compatibilizer was determined for this composition. The composition with the optimum compatibilizer was then studied in more detail for the mechanism of compatibilization.

The PET specimens tested at 100%/min displayed a yield maximum; however, the PE did not (Fig. 2). According to ASTM D638, the yield strength should be taken as a percent offset when there is no yield maximum. However, the 0.2 or 0.3% offset yield strengths resulted in values less than one half of the actual flow stress (Fig. 2). The 0.2% offset yield strength for PE would give a value of approximately 10 MPa, and the actual maximum flow stress is seen to be close to 22 MPa. Therefore, the yield strength was taken as the maximum flow stress for materials which displayed no yield maximum.

The uncompatibilized blends at 75 PET/25 PE and 50/50 did not exhibit yielding. Instead, they fractured in a brittle fashion. The 25 PET/75 PE

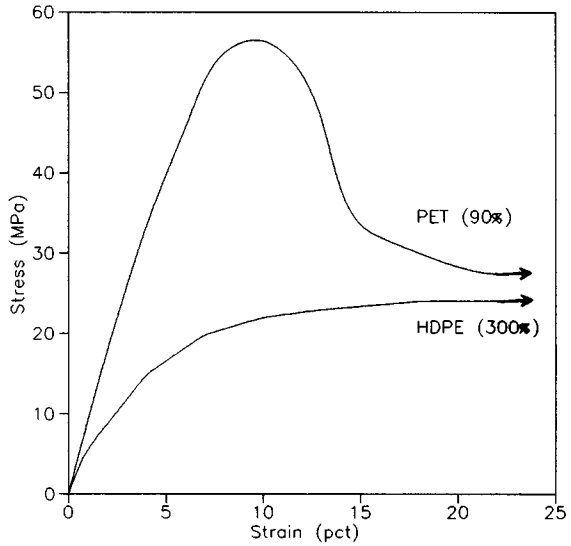

Figure 2 Initial section of the stress–strain curves showing that the 0.2 or 0.3% offset yield strength could not be used for some of the materials.

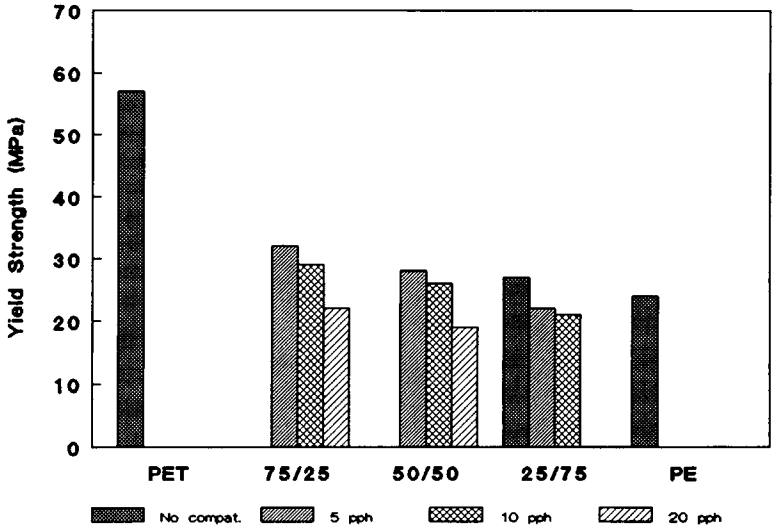

Figure 3 The resulting decrease in the yield strength due to increasing compatibilizer in all compositions.

blend does exhibit yielding at about 30 MPa, which is slightly lower than anticipated from the rule of mixtures (35 MPa). The yield strength for this blend decreases with the addition of 5 and 10 pph compatibilizer (Fig. 3). Similarly, the other two compositions displayed a decrease in yield strength with increasing compatibilizer.

The modulus of all compositions decreased slightly upon the addition of compatibilizer (Fig. 4). This is the expected result due to the compatibilizer's elastomeric character.

The ϵ_b did not markedly improve with the addition of the high viscosity SEBS at any composition. However, the ϵ_b improved considerably with the MA-*g*-SEBS in all compositions. The addition of MA-*g*-SEBS in the 25 PET/75 PE resulted in an ϵ_b of 440%, which is greater than that of PET (90%) or PE (300%) alone.

The modulus and yield strength did not change considerably with the additional compatibilizer. However, the compatibilizer caused a large difference in the ϵ_b of the blends, a property which more

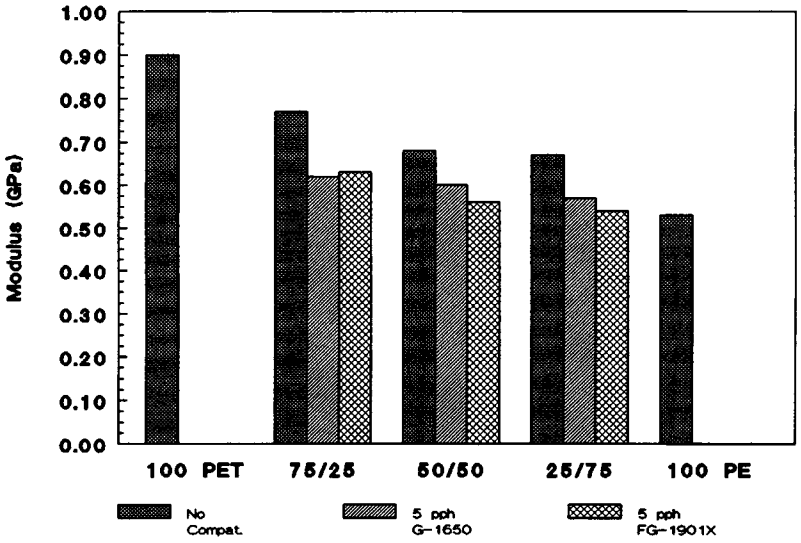

Figure 4 The modulus decreases with increasing compatibilizer in all compositions.

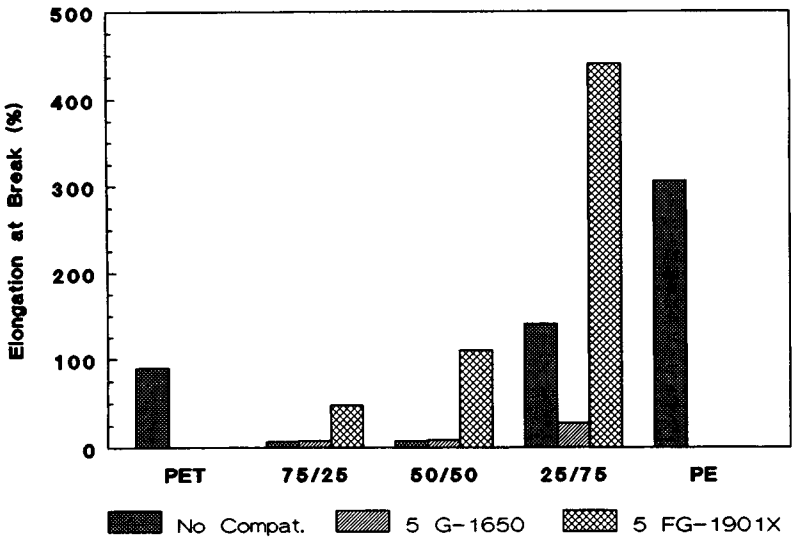

Figure 5 The elongation at break demonstrates that the 50/50 blend is the most sensitive to compatibilizer.

accurately reflects toughness and thus will be used to determine the effectiveness of the compatibilizer. In this regard, the relative values of ϵ_b are considered. That is, the ϵ_b of the compatibilized blend normalized by the ϵ_b of the uncompatibilized. As such, one may determine an index of compatibilization for each blend composition. The higher the index, the more efficient the compatibilizer is in toughening the blend. The ϵ_b's for all of these blend compositions are shown in Figure 5. For the 75 PET/25 PE blend the index was 7, for the 50 PET/50 PE blend 14, and for the 25 PET/75 PE blend 3. The 25/75 blend had the highest ϵ_b with the addition of compatibilizer, but the improvement over the uncompatibilized blend was not as large as for the 50/50. The 50/50 blend had the highest index of compatibilization and as a result was examined in more detail.

The three different SEBSs and the MA-*g*-PE were added to the 50/50 blend at 5, 10, and 20 pph to identify the best compatibilizer (Fig. 6). The high and low viscosity SEBS did not improve the ϵ_b considerably at any concentration. This is attributed to

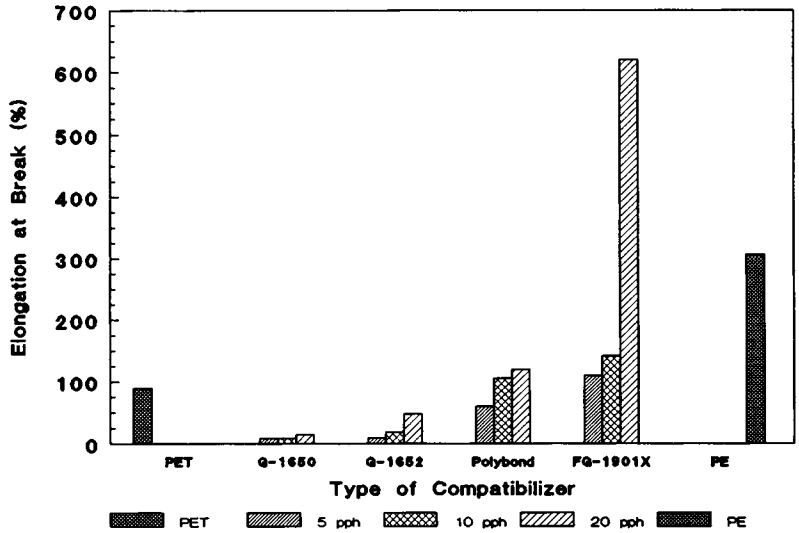

Figure 6 The elongation at break increases the most with the MA-*g*-SEBS (Kraton FG-1901X) at 20 pph.

Table I Results of an Exploratory Study on Strain Rate Dependence of 50/50/20 pph MA-*g*-SEBS Blend

Rate (%/min)	Modulus (GPa)	Yield Strength (MPa)	Tensile Strength (MPa)	Elongation at Break (%)
10	0.36	17	21	830
100	0.52	19	17	620
1000	0.61	24	19	70

the nonpolar nature of both block copolymers that results in little chance of strong interactions with the PET. The low viscosity SEBS was slightly better than the high viscosity SEBS, possibly resulting from better mixing. The larger increase in the ϵ_b associated with the addition of MA-*g*-PE is thought to be a result of more effective coupling between PE and PET. The anhydride will most likely interact with the carbonyl groups of the PET, whereas the ethylinic segment of the MA-*g*-SEBS may have interacted with the PE. If this was the only aspect considered, then the MA-*g*-PE would be expected to produce better properties than the MA-*g*-SEBS. However, this is not the case as seen in Figure 6, where the ϵ_b of the blend with MA-*g*-SEBS is considerably better than that of the blend compatibilized with MA-*g*-PE. The MA-*g*-SEBS has maleic anhydride grafted on the ethylene–butylene segment of the copolymer, but it also has segments which would be expected to not assist in compatibilization (i.e., styrene).

There are several possibilities as to why the MA-*g*-SEBS is a much more effective compatibilizer. One possibility could be the higher viscosity of the MA-*g*-PE not allowing for good mixing of the two phases. The viscosity was found using a constant shear stress of 678,000 N/m^2, the MA-*g*-PE was found to be higher (12,100 N s/m^2) than that of the MA-*g*-SEBS (10,900 N s/m^2). Another possibility is the fact that there is twice as much maleic anhydride in the MA-*g*-SEBS (2%) than there is in the MA-*g*-PE (1%), which may allow for more interaction with the PET. This compatibilizer was also found to be effective in our study of recycled scrap blends of PET/PE. The MA-*g*-SEBS was therefore the one used for further studies on these blends.

The maximum toughness in the 50 PET/50 PE blend was achieved at 20 pph MA-*g*-SEBS (Fig. 6). This 50/50/20 blend had a higher ϵ_b (600%) than either PET (90%) or PE (300%) alone and thus is coined "super tough." Paul and co-workers[1] also found increases in toughness with the addition of 20 pph low viscosity SEBS, from 3 to 200%. However, in their study, the strain rate used was half that of this study ($\sim$ 50%/min), and the improvements seen in their blend were not better than the constituent components. The MA-*g*-SEBS used in our study resulted in a much larger increase in toughness, from 7 to 600%, even though a higher strain rate was used (100%/min). An exploratory study on strain rate dependence was conducted on this blend, and the results are shown in Table I.

Phase Morphology

Because of inherent incompatibility of PE with PET, their blends produce two-phase materials. Hence, their morphology plays a primary role in determining the resulting properties. In such a system, the compatibilizer acts in the melt to couple the various phases and to produce a beneficial phase morphology by lowering the interfacial tension.[12,13] Consequently, a systematic examination of the morphological evolution is necessary to rationalize the obtained improvements in mechanical performance.

Morphological analysis of multiphase blends should define the size, orientation, and distribution of the dispersed phase, the nature of the interphase, and how the compatibilizer alters these features. An important question in this regard is the role of the compatibilizer in reconstituting the microstructure at the interphase. Additionally, in our case, the crystallinity of the two major components must be examined. This is particularly important since PET could exhibit wide crystalline variance, which results in a major change in mechanical properties.[14] Finally, the origin of improved mechanical performance can be defined by examining the role played by the coexisting domains (continuous phase, dispersed phase, and the interphase) in load bearing and in inducing irreversible deformation processes.

The above analytical strategy is focused on the 50/50/20 blend in lieu of its superior toughness (Fig. 6). Its morphological characteristics will be contrasted with those of the uncompatibilized 50/50 blend to understand the compatibilization effects.

Figure 7 is a SEM micrograph of the uncompatibilized 50/50 blend that was cryogenically fractured perpendicular to the injection direction. The dispersed phase exists as irregular domains ranging in size from 2 to 20 μm. The identity of the continuous phase cannot be readily determined from this figure in view of the equal amounts of the two phases (50/50 blend). To facilitate identification of the

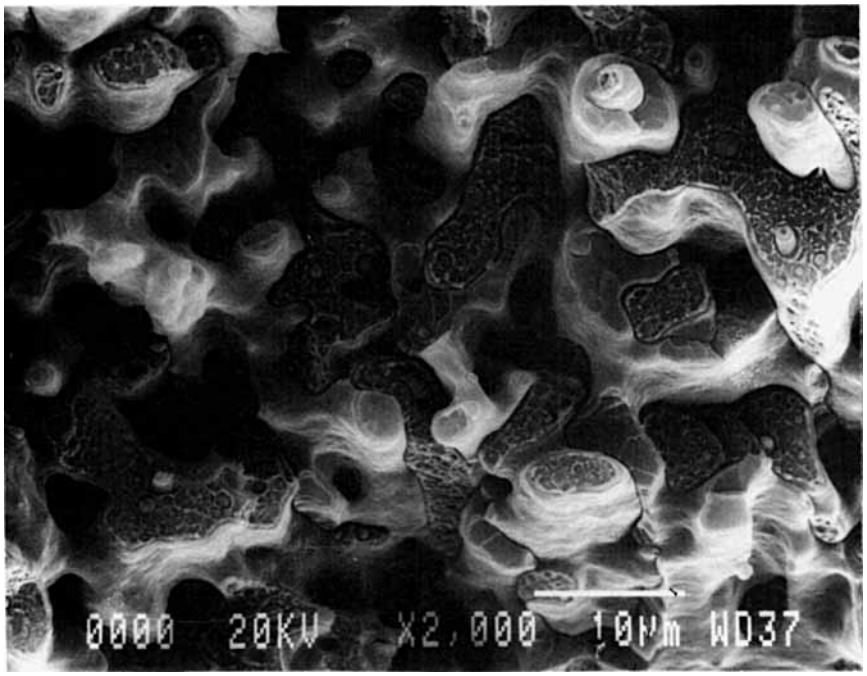

Figure 7 SEM micrograph of 50/50 blend with no compatibilizer perpendicular to injection direction showing undeformed morphology (×2000).

continuous phase, we examined a 75/25 blend in which PET constitutes the major (continuous) phase. Comparison of these morphologies showed a clear similarity of the dispersed domains in both blends. The dispersed phase in the 75 PET/25 PE blend is the PE. This comparison suggests that PET is the continuous phase in the 50/50 blend (Fig. 7). The morphology of the dispersed phase (PE) in both the 75/25 and 50/50 blends seems to be a multidomain in that it contains smaller, well-defined domains (subphase). Obviously, the smaller particles within the PE domains cannot be PE, but must be PET. That is why they are classified as a "subphase."

The subphase morphology is known to exist in HIPS,[15] where subphase separation occurs during polymerization of polystyrene in the presence of butadiene. The origin of the subphase in PET/PE is, however, different. In a related study,[2] it is reported that the subphase morphology in PET/PE originated from small PE particles surrounded by another material. They assumed that this material was the elastomer since it is the component most easily strained. Nevertheless, this same type of subphase morphology appears also in our 50/50 blend (Fig. 7), which contains no elastomer. This observation refutes the origin of the subphase morphology suggested by Chen and Shiah.[2]

A plausible mechanism for the formation of subphase domains may be as follows: As the molten blend cools below the melting range of PET (260–220°C), most of it solidifies as the continuous phase. Small amounts of PET in droplet form could have remained entrapped within the PE melt, which subsequently constitute the subphase.

If the PET is crystalline, these two phases may be seen as two crystallite sizes. The DSC trace of PET is shown in Figure 8 and shows the glass transition (T_g) of PET at 77°C, its cold crystallization (T_c) at 130°C, and its melting peak (T_m) at 250°C. The percent crystallinity of the PET was obtained by subtracting the area of the cold crystallization peak from the area of the PET melt peak and dividing by 117 J/g, the heat of fusion of PET.[16] This was normalized by the respective temperatures of the transitions. This analysis indicates that the PET existed in an amorphous state in the injection molded bars.

The thermogram in Figure 9 is of PE and the T_m of PE was at 130°C. The percent crystallinity of PE was found by dividing the area under the melting peak of PE by the heat of fusion of PE, 276 J/g.[17] The percent crystallinity was found to be approximately 58% for PE. The T_m of PE coincides with the T_c of PET, and therefore the crystallinity of PET in the blends could not be determined from DSC.

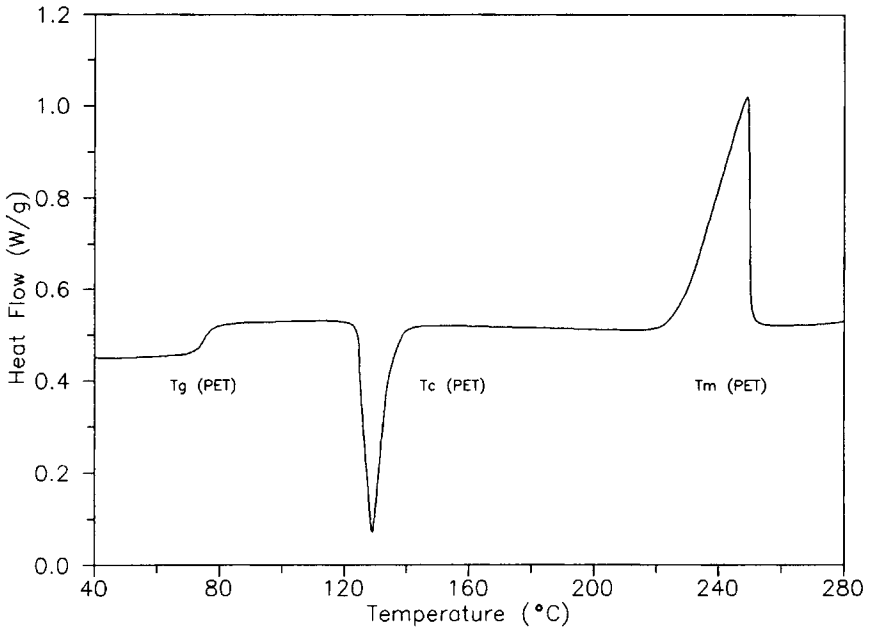

Figure 8 DSC trace of PET showing the glass transition, cold crystallization, and melting temperatures.

The thermogram of uncompatibilized 50/50 blend is seen in Figure 10, in which the coincidence of the peaks is seen to have eradicated the cold crystallization peak of PET.

Wide angle X-ray diffraction (WAXD) was then used for determining crystallinity in the blends. It was confirmed that the PET in the blend in the injection molded form is amorphous. This was found by the lack of crystalline PET peaks in the diffractometer scan of the 50/50 blend (Fig. 11). The peaks seen at 21.55°, 23.89°, 30.01°, and 36.2° (2θ) are due to the crystalline PE.

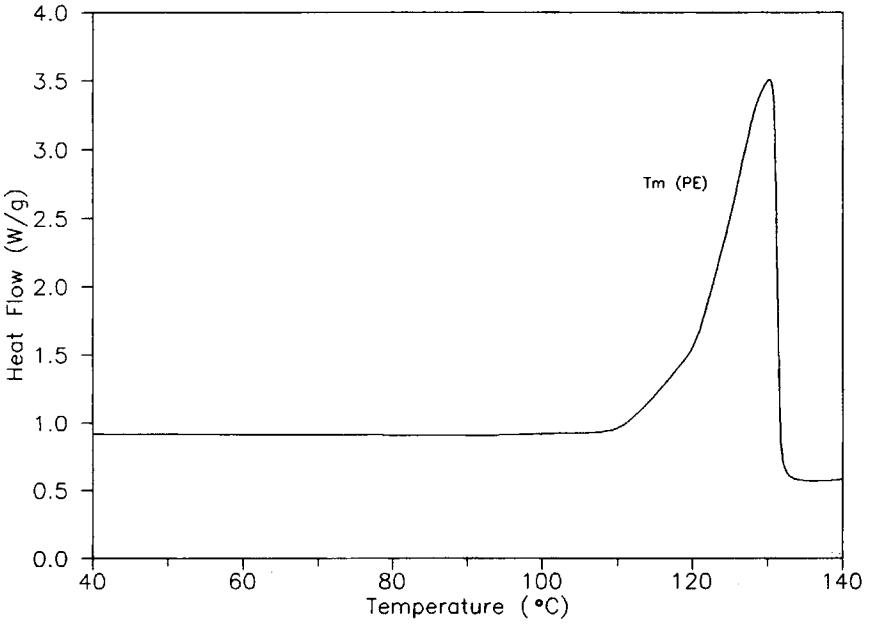

Figure 9 DSC trace of PE showing the melting temperature of the PE.

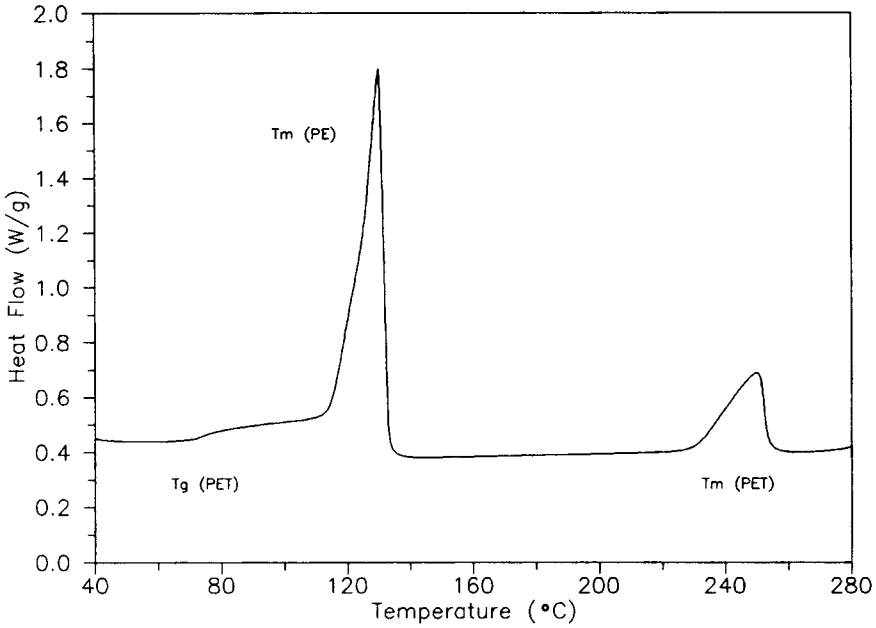

Figure 10 DSC trace of 50/50 blend without compatibilizer, showing only one melting peak for PET, indicating only one crystallite size.

Upon compatibilization phase inversion appears to have occurred in the 50/50/20 blend (Fig. 12). PET now appears as the discontinuous phase (PET islands) in a continuous matrix exhibiting a multidomain morphology. This could be due to the aforementioned PET melt solidifying process being

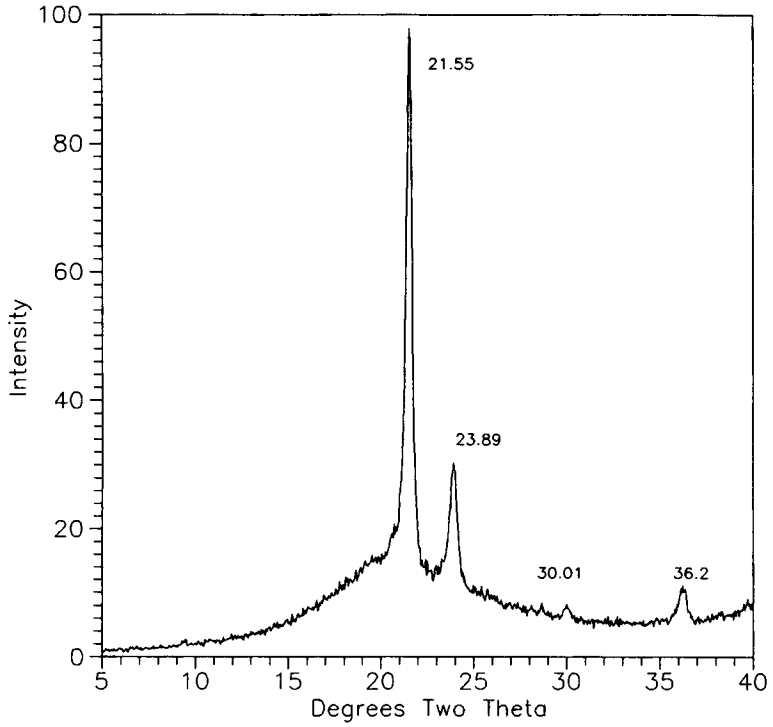

Figure 11 WAXD of a 50/50 blend showing the lack of PET crystalline peaks and crystalline peaks of PE at 21.5, 23.89, 30.01, and 36.2.

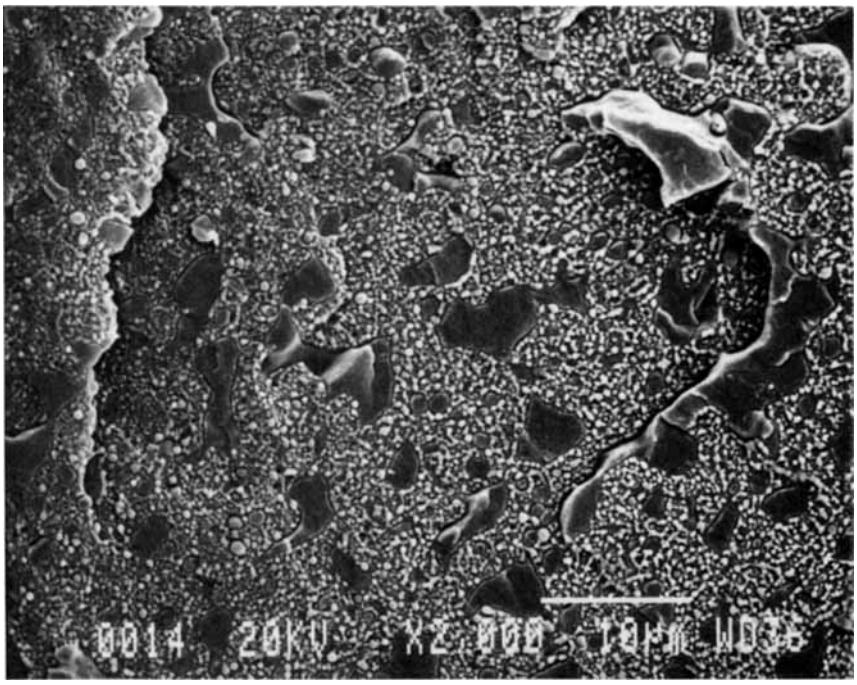

Figure 12 SEM micrograph of undeformed 50/50/20 pph MA-*g*-SEBS perpendicular to injection direction showing phase inversion (×2000).

further enhanced due to the addition of the MA-*g*-SEBS, which reduces the melt viscosity. As a result, more PET is dispersed as a subphase (Fig. 12), causing phase inversion in the blend. Further indication of an increase in the PET subphase is the fact that the discontinuous phase (PET islands)

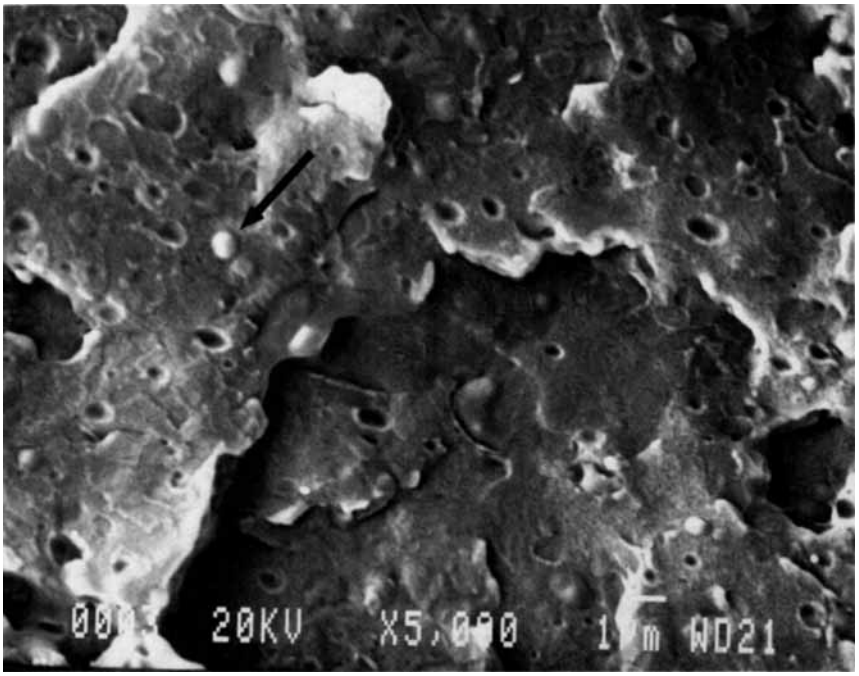

Figure 13 SEM micrograph of PET/20 pph MA-*g*-SEBS perpendicular to injection direction showing spherical particles well-adhered to the PET matrix (×5000).

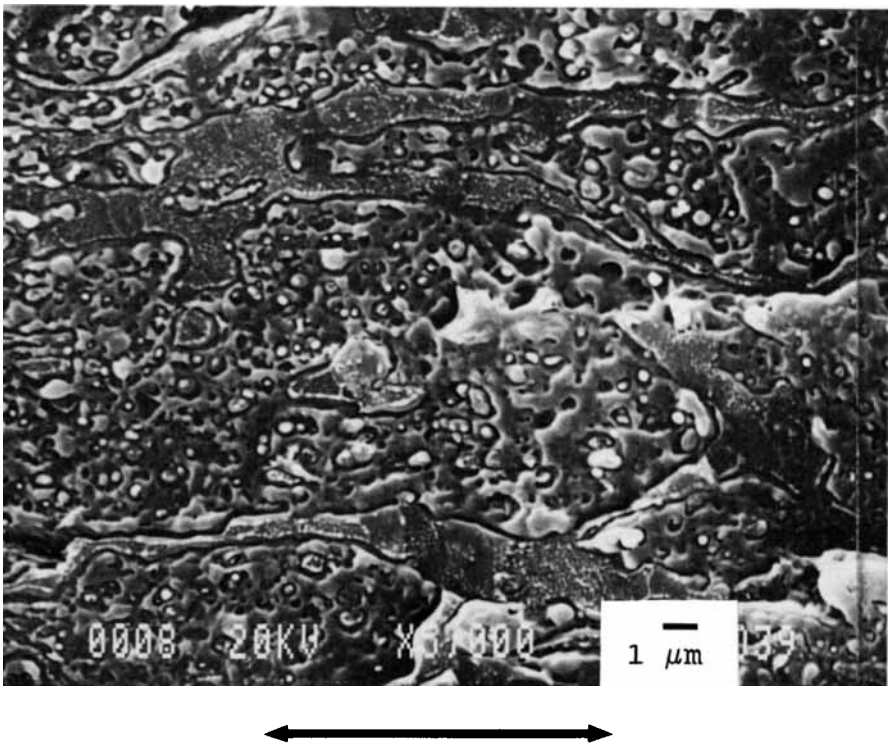

Figure 14 SEM micrograph of undeformed 50/50/20 pph MA-*g*-SEBS parallel to injection direction displaying orientation of PET, arrow indicates injection direction (×5000).

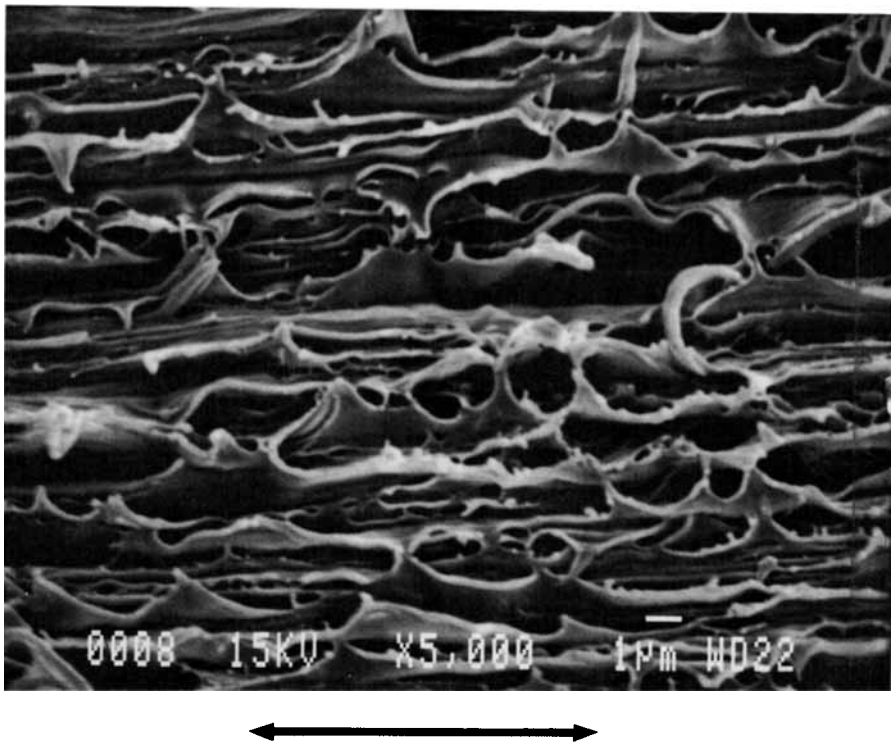

Figure 15 SEM micrograph of 50/50/10 pph MA-*g*-SEBS in the neck parallel to deformation direction showing 1–3 μm gaps; the arrow indicates deformation direction (×5000).

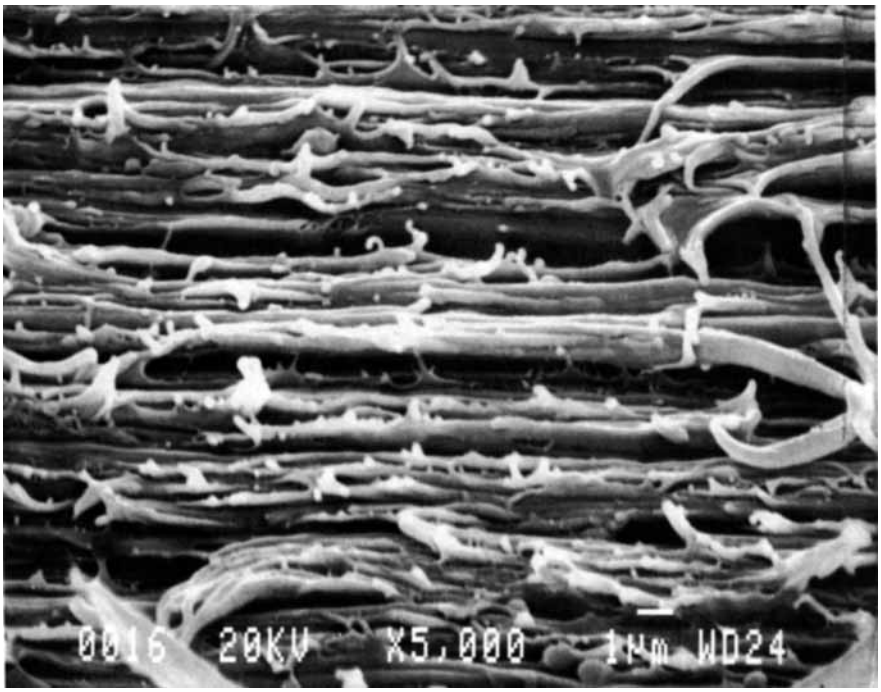

Figure 16 SEM micrograph of 50/50/20 pph MA-*g*-SEBS in the neck parallel to deformation direction showing 1 μm or smaller gaps; the arrow indicates deformation direction (×5000).

does not make up 42% (50 pph) of the material; image analysis has shown that the discontinuous phase actually makes up approximately 24%. The discontinuous phase ranges in size from 1 to 10 μm, with the majority being 5 μm or smaller. In comparing the compatibilized blend (Fig. 12) to the uncompatibilized blend (Fig. 7), it is clear the addition of compatibilizer reduces the phase size for both the PET domains and the particulate subphase. As will be seen later, the subphase morphology plays a major role in providing super tough behavior in this compatibilized blend.

Even though the MA-*g*-SEBS constitutes about 17% (20 pph) in the blend of Figure 12, it cannot be identified as a separate phase. Higher magnification of selected areas in Figure 12 did not reveal a physical interphase. To explore the role played by the compatibilizer, a blend containing 20 pph MA-*g*-SEBS was prepared with the PET (no PE) using the same extrusion and molding conditions. The injection-molded tensile bars were cryogenically fractured perpendicular to the injection direction. A separate MA-*g*-SEBS phase could be identified as spherical particles about 1 μm in diameter. The particles appeared to be well-adhered to the PET matrix (Fig. 13). Image analysis revealed that the particulate phase was 7% of the area, which constitutes less than half of the expected 17% (20 pph) in the blend. There appears to be a gradient of coexistence of PET and MA-*g*-SEBS possibly from the molecular level to the micro level. The fact that in the 50/50/20 blend there is significantly less PET than expected (Fig. 12) further suggests that the PET may be coexisting with the MA-*g*-SEBS at a submicron level. Thus, it is assumed that the MA-*g*-SEBS must have interacted with the PET through its anhydride groups to form a partially miscible blend of reduced viscosity.

Domain orientation in a blend is an important morphological factor which affects the material properties. Figure 14 is a photomicrograph of the 50/50/20 blend that was cryogenically fractured in the injection direction. In this micrograph, orientation and interconnectivity of the PET phase (PET islands) is evident. On the other hand, the PE-rich matrix remains unoriented.

Deformation Mechanisms

The constituent materials in this blend had ϵ_b of 90% (PET) and 300% (PE). When blended at a

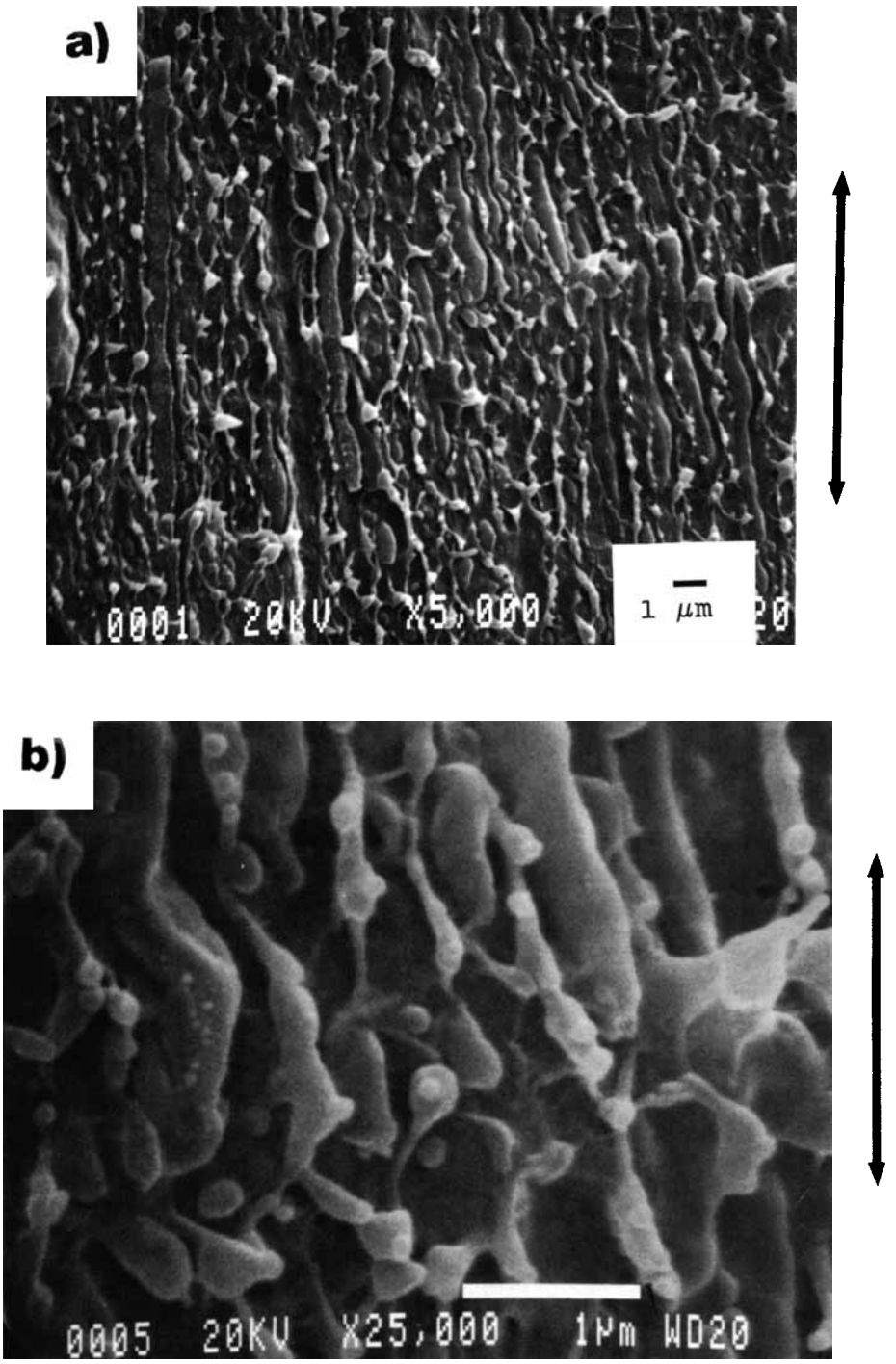

Figure 17 (a) SEM micrograph of 50/50/20 pph MA-*g*-SEBS in the shoulder of the neck parallel to deformation direction showing alignment of all phases in the tensile direction (×5000). (b) Magnified micrograph of 17(a) showing orientation at the 100 nm scale; the arrow indicates deformation direction (×25,000).

1 : 1 ratio, the ϵ_b dropped dramatically to 7%. However, with the addition of only 20 pph MA-*g*-SEBS, an ϵ_b of 600% was achieved, higher than either of the two constituent materials. The mechanisms of irreversible deformation were examined to discover the morphological source of the toughening.

SEM micrographs were taken in the necked region (deformation direction) of the 50/50 blends with 10 and 20 pph MA-*g*-SEBS (Figs. 15 and 16). The phases are smaller in the 20 pph blend and have elongated to a point where the PET phases cannot be discerned from the PE phases. Between the phases there appears to be bridges that allow both phases to become load-bearing and to deform co-continuously (Figs. 15 and 16). The bridges seen in the 20 pph blend are smaller, and fewer gaps are seen in this blend. These bridges were also found in compatibilized nylon 6/PE blends and have been found to be the MA-*g*-SEBS.[18]

Next, sections were made in the shoulder of the neck in the deformation direction. In this initial portion of the neck both phases of the undeformed morphology are becoming aligned in the tensile direction [Fig. 17(a)]. At higher magnification it is seen that this orientation is apparent even at a 100 nm scale [Fig. 17(b)]. This orientation on the nano scale shows that the material is compatibilized to a degree where both phases are deforming near the molecular level. This result is unusual for a compatibilized blend. The theory of compatibilization usually described occurs at the micron scale and involves adhesion between the two principle phases by the compatibilizer. The morphology and deformation mechanisms of this blend make it different from the current two-phase blend technology.

CONCLUSIONS

This study examined a number of block copolymers and a maleinated polyethylene for roles as compatibilizers of PET/PE blends of varying compositions. MA-*g*-SEBS was found to be the most effective compatibilizer. The main conclusions derived from this study are:

1. The compatibilized blend exhibited a co-continuous morphology in which an oriented PET phase was dispersed into a multidomain network matrix of PE, PET, and MA-*g*-SEBS.
2. A 50 PET/50 PE/20 pph MA-*g*-SEBS blend exhibited an elongation at break which outperformed PET more than fivefold and PE twofold; thus the blend was identified as "super tough."
3. Superior toughness was attributed to the ability of all the domains to bear load cooperatively allowing irreversible deformation to occur down to the nano scale.

This research is supported by the Edison Polymer Innovation Corp. (EPIC). The blending experiments were conducted at the EPIC-M. A. Hanna Polymer Blending and Compounding Center. The authors are indebted to Professor J. L. White for guiding the blending study. We are also grateful to Mr. Dong-Joon Ihm for preparing the blends.

REFERENCES

1. T. D. Traugott, J. W. Barlow, and D. R. Paul, *J. Appl. Polym. Sci.*, **28,** 2947 (1983).
2. I. M. Shen and C.-M. Shiah, *SPE ANTEC '89,* 1802 (1989).
3. J. Curry and A. Kiani, *SPE ANTEC '90,* 1452 (1990).
4. G. E. Wissler, *SPE ANTEC '90,* 1434 (1990).
5. A. Khelifi and F. Lai, *SPE ANTEC '88,* 1824 (1988).
6. L. A. Utracki, *Polymer Alloys and Blends: Thermodynamics and Rheology,* Oxford University Press, New York, 1990.
7. T. L. Carté, Master's thesis, Case Western Reserve University, 1992, Chap. 2.
8. A. Y. Coran and R. Patel, *J. Appl. Polym. Sci.,* **20,** 3005 (1976).
9. D. R. Paul and S. Newman, Eds., *Polymer Blends,* Academic, New York, 1978, Vol. 2.
10. G. Serpe, J. Jarrin, and F. Dawans, *Polym. Eng. Sci.,* **30,** 553 (1990).
11. S. Wu, *Polymer,* **26,** 1855 (1985).
12. C. Chen, E. Fontan, K. Min, and J. L. White, *Polym. Eng. Sci.,* **28,** 69 (1988).
13. M. Xanthos, *Polym. Eng. Sci.,* **28,** 1392 (1988).
14. M. J. Napolitano and A. Moet, *J. Appl. Polym. Sci.,* **32,** 4989 (1986).
15. C. B. Bucknall, *Toughened Plastics,* Applied Science, London, 1977.
16. C. W. Smith and M. Dole, *J. Polym. Sci.,* **20,** 37 (1956).
17. B. Wunderlich and M. Dole, *J. Polym. Sci.,* **24,** 201 (1957).
18. R. Armat and A. Moet, to appear.

Received July 1, 1992
Accepted July 17, 1992